Optically Detected Magnetic Resonance of the Phosphorescent Bases of *Escherichia coli* Valine-Specific Transfer Ribonucleic Acid†

Mohammad-Reza Taherian* and August H. Maki

ABSTRACT: Phosphorescence spectroscopy and optical detection of triplet state magnetic resonance (ODMR) spectroscopy have been used to characterize bases that contribute to the phosphorescence emission of *Escherichia coli* valine-specific transfer ribonucleic acid. When it is excited with 335-nm light, a short-lived phosphorescence with an origin near 435 nm is observed and is assigned to 4-thiouridine (s^4U) at position 8 of the tRNA sequence. With excitation at 290–300 nm, a structured, long-lived phosphorescence is observed with an origin near 380 nm, in addition to the s^4U phosphorescence. Comparison was made of the phosphorescence and ODMR spectra between Mg^{2+}-containing and Mg^{2+}-free tRNA samples. The s^4U phosphorescence of the Mg^{2+}-containing sample is more structured, and the peak is blue shifted relative to the Mg^{2+}-free sample. Both samples give a single low-frequency (ca. 2.9 GHz) ODMR signal, but the high-frequency signal region (ca. 19–20 GHz) is structured. The Mg^{2+}-containing sample has a partially resolved group of lines centered at 19.3 GHz, whereas the Mg^{2+}-free sample has two broad bands centered at 19.2 and 20.0 GHz. The differences are attributed to effects of Mg^{2+} on the tRNA conformation. The ODMR signals observed by monitoring the long-lived phosphorescence are assigned to a pyrimidine nucleoside, possibly 5-(carboxymethoxy)uridine in the anticodon.

4-Thiouridine (s^4U)[1] is a common minor base in *Escherichia coli* tRNA (Singhal & Fallis, 1979). Except for a few examples in which position 8 from the 5′ end contains uridine (U), all the other *E. coli* tRNAs studied have s^4U at this position. $tRNA^{Tyr}$, in particular, has an additional s^4U at position 9 (Doctor et al., 1969). The function of this nucleoside is not very well understood (McCloskey & Nishimura, 1977), though there is evidence that it does not play a critical role in the major functions of tRNA, namely, aminoacylation and protein synthesis (Walker & RajBhandary, 1970). On the other hand, s^4U has its own interesting spectroscopic properties, with some unique features such as the low energy of its first excited triplet state relative to other bases of tRNA which make the spectroscopy of this base a natural choice for the investigation of structural problems related to tRNA. Lack of known biochemical activities has not impeded spectroscopists in using this base as a probe to study the structural properties of tRNA (Hélène et al., 1968; Hélène & Yaniv, 1970; Shalitin & Feitelson, 1973, 1976a,b).

Valine-specific tRNA from *E. coli* is one of the most extensively studied biopolymers in its class. A cloverleaf structure of this molecule showing the location of s^4U, along with the Watson–Crick (secondary) base pairs, is shown in Figure 1. Position 8 is located between the double helices of the CCA and dihydro-U stems and is considered to be strategically important (Teeter et al., 1980). It has been suggested that because of this important location, s^4U can serve as a useful intrinsic phosphorescence probe (Shalitin & Feitelson, 1976a).

Soon after the discovery of this minor base in tRNA molecules, phosphorescence emission at 77 K was used (Hélène et al., 1968; Hélène & Yaniv, 1970) to show the feasibility of this method to detect the presence of s^4U in the complex structure of biopolymers. Room temperature studies showed an emission peaked at 550 nm from s^4U, both as a free base and as a component of the tRNA structure (Shalitin & Feitelson, 1973, 1976a,b; Ponchon et al., 1971). Below the freezing point of the solution a second peak at 475 nm appears, which becomes the most prominent band as the temperature is lowered (Shalitin & Feitelson, 1973). It was suggested that the room temperature emission originates from a triplet state of lower energy than the normal s^4U triplet state, but its nature is not yet understood.

High-resolution NMR studies on $tRNA^{Val}$ have shown the existence of tertiary base pairing between s^4U at position 8 and adenosine at position 14 (Reid & Robillard, 1975; Wong & Kearns, 1974; Wong et al., 1975). Also, ultraviolet irradiation of aqueous solutions of tRNA leads to photochemical cross-linking between s^4U at position 8 and cytidine at position 13 (Favre et al., 1969).

The low energy of the s^4U triplet and singlet states makes this molecule a natural acceptor for energy transfer from normal as well as from other minor bases. Many of the tRNA bases are involved in secondary base pairing, which is known to quench singlet and triplet energy (Steiner et al., 1967), but there are still several bases which can, in principle, transfer their energy to s^4U. A study of the room temperature phosphorescence excitation spectrum of s^4U and the 8–13 photocross-linking action spectrum of $tRNA_1^{Val}$ (Ballini et al., 1976) showed the importance of singlet–singlet (S–S) energy transfer from the normal bases. Critical Förster distances for energy transfer were calculated by using fluorescence quantum yields of common bases and the absorption spectrum of s^4U. In the absence of crystal structure information on $tRNA_1^{Val}$ the coordinates of yeast $tRNA^{Phe}$ (Kim et al., 1974; Robertus et al., 1974) were used to search for bases within critical range. If a 50% efficiency due to the orientational factor is assumed, an estimated five to six bases had to be involved in order to explain the excitation spectrum. There is also the possibility of multiple step S–S energy transfer, which is a channel for

† From the Department of Chemistry, University of California, Davis, California 95616. *Received April 1, 1981.* This work was partially supported by a research grant (CHE 79-10394) from the National Science Foundation.

[1] Abbreviations used: s^4U, 4-thiouridine; m^1s^4U, 1-methyl-4-thiouracil; $m^1m^3s^4U$, 1,3-dimethyl-4-thiouracil; U, uridine; cmo^5U, 5-(carboxymethoxy)uridine; DTT, dithiothreitol; EGW, ethylene glycol–water; ODMR, optical detection of (triplet state) magnetic resonance; ZFS, zero-field splittings; NMR, nuclear magnetic resonance; m^1s^2U, 1-methyl-2-thiouracil; $m^1s^2s^4U$, 1-methyl-2,4-dithiouracil; EDTA, ethylenediaminetetraacetic acid, m^1U, 1-methyluracil.

0006-2960/81/0420-7295$01.25/0

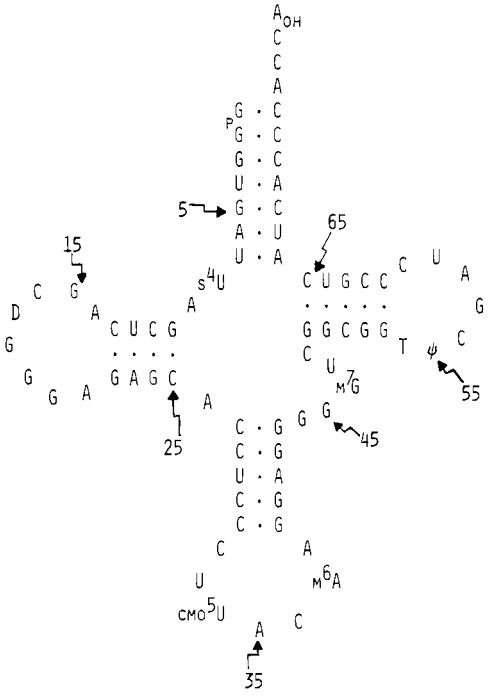

FIGURE 1: Cloverleaf structure of $tRNA_1^{Val}$ from *E. coli*. Sequence from Gauss et al. (1979).

more distant bases to participate in energy transfer. It appears probable that most of the excitation energy in the vicinity of s^4U, which is not quenched as a result of base pairing, is emitted through this minor base. This includes most of the molecule with the exception of the anticodon loop.

We have recently used ODMR to obtain the ZFS parameters of m^1s^4U, m^1s^2U, and $m^1s^2s^4U$ for the first time (Taherian & Maki, 1981). The ZFS parameters are found to be unexpectedly large, probably the result of spin–orbit coupling introduced by the relatively massive S atom.

In this study we will use ODMR to study the triplet state of s^4U both as a free nucleoside and as a constituent of $tRNA_1^{Val}$. A comparison of these should help us to evaluate the possible role of ODMR spectroscopy of s^4U as a structural method. In this application, some of the triplet state parameters may be more sensitive to environmental changes than others. We will also be interested in explaining the nature of the $tRNA_1^{Val}$ phosphorescence and in evaluating the contribution of nucleosides other than s^4U to the emission.

Materials and Methods

E. coli $tRNA_1^{Val}$ was obtained from Boehringer Mannheim as the lyophilized powder. It was from strain *E. coli* MRE 600, the sequence of which was shown by ribonuclease T_1 fragmentation (P. R. Schimmel, personal communication) to be similar to that of the *E. coli* K12 (Yaniv & Barrell, 1969). A Mg^{2+}-free sample was prepared by dissolving the lyophilized powder in doubly distilled deionized water and heating to 80 °C for ~0.5 h. At 52 °C the tertiary structure involving s^4U melts (Hélène et al., 1968), while at the temperature used here all the secondary structure of tRNA melts completely (Crothers et al., 1974). The solution was cooled slowly to room temperature in the course of ~1 h, and it was subsequently dialyzed against EDTA solution (10 mM) for 24 h at room temperature. This was followed by dialysis against a Mg^{2+}-free cacodylate buffer (30 mM, pH 6.8) for 2 days at the same temperature.

Mg^{2+}-containing samples were prepared by dissolving the lyophilized tRNA powder in $MgCl_2$ solution (10 mM). The solution was then heated to 80 °C for ~1 h, cooled over a period of ~1 h, and finally dialyzed against Mg^{2+}-containing cacodylate buffer for 2 days at room temperature.

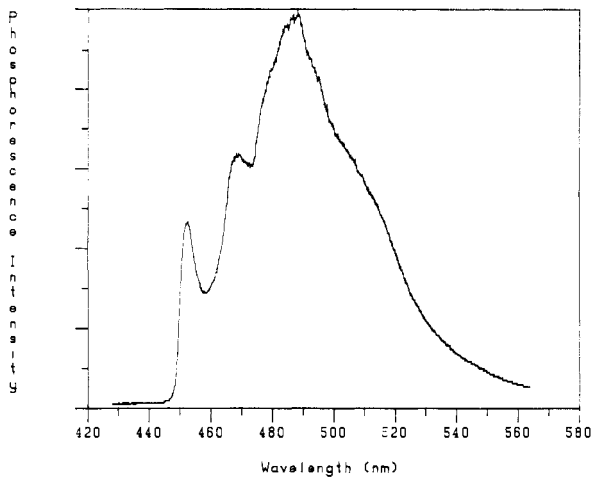

FIGURE 2: Phosphorescence spectrum of s^4U (ca. 0.2%) in U host crystal. Sample is excited at 365 nm at 4.2 K. The spectrum is monitored with a monochromator slit width of 1.6 nm.

The solutions so prepared were kept in the refrigerator at −5 °C in the dark and were mixed with equal volumes of ethylene glycol (Matheson Coleman and Bell, chromatography grade) before being transferred to 1-mm i.d. quartz sample tubes for measurement. The sample concentrations were measured by recording the UV absorption spectrum. Using $A_{260} = 6.3 \times 10^5$ (Eisinger, 1971), we calculated the concentration to be 6.4×10^{-5} M in tRNA. On the other hand, using a molar extinction coefficient of 1.64×10^3 for the 335-nm absorption band of s^4U (Elion et al., 1946), we calculated the concentration to be 4.2×10^{-5} M.

4-Thiouridine was purchased as uridine 4,4′-disulfide from Sigma. The aqueous solution (10^{-4} M) was reduced with a 10-fold excess of dithiothreitol (DTT) and was then mixed with an equal volume of ethylene glycol prior to use for spectroscopic measurements. The cocrystallized sample of s^4U in U (P-L Biochemicals) was prepared by addition of an excess of DTT to the appropriate alcoholic solution of s^4U and U. The solvent was evaporated over P_2O_5 in a desiccator in the dark. The ratios of s^4U and U were chosen so that the crystalline sample would contain either ~0.5% or ~0.2% s^4U.

The ODMR spectrometer has been described previously (Maki et al., 1978; Maki & Co, 1976; Taherian & Maki, 1981). The low-frequency microwaves (<18 GHz, ~10 mW) were transmitted through a coaxial cable to the sample held in a copper helix (3-mm i.d.). Microwaves in the 18–26.5-GHz band (~10 mW) were transmitted through a stainless steel waveguide to the sample. The sample was held in a stainless steel helix (3-mm i.d.) soldered to the open end of the waveguide (Taherian & Maki, 1981). During the course of the phosphorescence or ODMR measurements, the sample was kept at pumped helium temperature (ca. 1.1 K), unless otherwise noted. The sample was excited with a 100-W high-pressure mercury arc whose output was passed through an aqueous IR filter, a monochromator with ca. 10-nm band-pass, and an order-sorting glass filter (Corning 7-54).

Results

(A) Phosphorescence Spectra. The phosphorescence spectrum of s^4U in polycrystalline U is shown in Figure 2. The emission is characterized by a vibrational progression of ca. 770 cm^{-1}, which is close to that observed from m^1s^4U as a guest in m^1U (Taherian & Maki, 1981). s^4U in an ethylene gly-

Table I: Zero-Field ODMR Frequencies of 4-Thiouridine and *E. coli* $tRNA_1^{Val}$ [a]

	λ_{exc} (nm)	λ_{obsd} (nm)	ν_1 (GHz) [$\Delta\nu_1$ (MHz)]	ν_2 (GHz) [$\Delta\nu_2$ (MHz)]	ν_3 (GHz) [$\Delta\nu_3$ (MHz)]	$\lvert D\rvert$ (cm^{-1})	$\lvert E\rvert$ (cm^{-1})
m^1s^4U in m^1U	365	447.5	3.00 [4.4]	16.57 [110]	19.70[b] [100]	0.605	0.0500
s^4U, 0.5% in U	365	452	3.433[c] [30]	16.2[d] [160]	19.8 [500]	0.600	0.0573
s^4U in 50% EGW	335	466.5	2.9 [300]		20[e] [900]	0.6	0.048
$tRNA_1^{Val}$, Mg^{2+}-containing solution	335	465	2.95 [450]		19.3[f]	0.59	0.049
	300[g]	440, 465	0.71[d] [120]	5.6[d] [950]			0.012
$tRNA_1^{Val}$, Mg^{2+}-free solution	335	465	2.90 [300]		20.0 [550]	0.62	0.048
					19.2 [550]	0.59	0.048
	300[g]	440, 465	0.69[d] [150]	5.2 [300]			0.012

[a] Signals are an increase in intensity unlesss otherwise indicated. Data for m^1s^4U are from Taherian & Maki (1981). [b] Two peaks split by 100 MHz. Average frequency is given. [c] A second signal occurs at 2.779 GHz having $\Delta\nu$ = 30 MHz. [d] Decrease in intensity. [e] Extremely weak signal. Only approximate peak is given. [f] Poorly resolved multiplet with individual line widths ca. 200 MHz. See Figure 5A. [g] New signals observed with 300-nm excitation are assigned to cmo^5U.

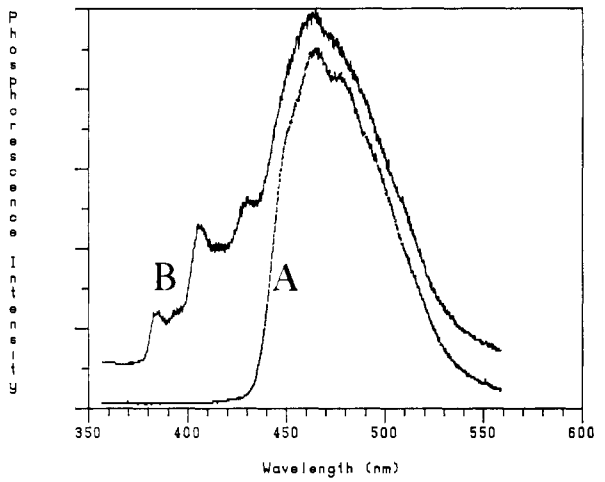

FIGURE 3: Phosphorescence spectra of $tRNA_1^{Val}$ in EGW (50% v/v). Solution contains $MgCl_2$ and cacodylate buffer (pH 6.8). The spectra are taken at 1.1 K with an emission monochromator slit width of 1.6 nm. (A) Excitation wavelength is 335 nm. (B) Excitation wavelength is 290 nm.

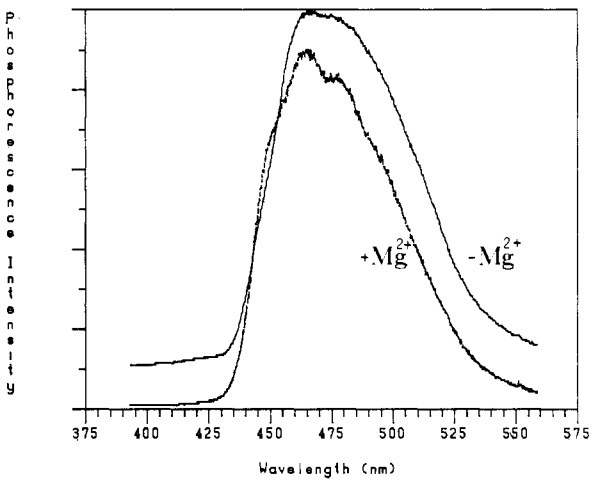

FIGURE 4: Superposition of 4-thiouridine phosphorescence spectra from $tRNA_1^{Val}$ at 1.1 K in ethylene glycol–cacodylate buffer mixtures (50% v/v; pH 6.8) in the presence and absence of Mg^{2+}.

col–water (EGW) solvent mixture shows a structureless spectrum resembling the previously reported emission (Hélène et al., 1968; Hélène & Yaniv, 1970). The origin of the phosphorescence in EGW occurs at 445 nm, which is the same as that of the crystalline emission, within the experimental uncertainty.

Phosphorescence spectra of the $tRNA_1^{Val}$ sample in the Mg^{2+}-containing solution are given in Figure 3. The Mg^{2+}-free sample shows a similar behavior. Figure 3 contains two spectra at different excitation wavelengths (335 and 290 nm) that have been recorded under otherwise identical experimental conditions. As can be seen from Figure 3, the spectrum is complex, and a variation in excitation wavelength helps to selectively excite different bases in the biopolymer. Excitation at 335 nm in both Mg^{2+}-free and Mg^{2+}-containing samples gives rise to a short-lived emission which is characteristic of s^4U (Hélène et al., 1968; Hélène & Yaniv, 1970). This emission is broader and less structured in the Mg^{2+}-free sample. A superposition of these spectra is shown in Figure 4, which clearly demonstrates a major red shift of the intensity in the spectrum of the Mg^{2+}-free sample.

Higher energy photons (λ_{exc} = 290–300 nm) excite other bases in the molecule and produce a long-lived phosphorescence component with an origin near 380 nm. Even though this is a common feature of both Mg^{2+}-containing and Mg^{2+}-free samples, the intensity of the long-lived phosphorescence of the Mg^{2+}-free sample is higher while its resolution is lower. Excitation at 290 nm where s^4U does not absorb significantly (Elion et al., 1946) helps to demonstrate the importance of energy transfer from other bases of tRNA since a considerable s^4U contribution to the phosphorescence is observed.

(B) ODMR. The ODMR frequencies of s^4U in the U host crystal and in ethylene glycol–water (EGW) glass are presented in Table I. All three transition frequencies of s^4U in the host crystal are very close to those observed previously (Taherian & Maki, 1981) for m^1s^4U in m^1U, indicating the similarity of the chromophores involved in the excited triplet state. The only major difference, other than multiple resolved peaks, is an inversion in the polarity of the ν_2 signal, which is a decrease in light intensity, whereas it is an increase in the case of m^1s^4U in m^1U.

In EGW, only two of the signals are seen, which are assigned on the basis of their frequencies to the ν_1 and ν_3 transitions of s^4U. The signals are very weak in this solvent. In general the ν_2 signal of s^4U is much weaker than the other two signals and since no signal was seen at frequencies around 23 GHz, we conclude that the ν_2 signal is in the 16-GHz region but is too weak to be detected.

In Table I, we list the frequencies of the ODMR transitions of the $tRNA_1^{Val}$ samples. The intermediate frequency signal of s^4U in $tRNA_1^{Val}$ also was not seen. Since this transition is observed both from s^4U in U and from m^1s^4U in m^1U host crystals, and also since the frequencies of the remaining two transitions are very close to the ν_1 and ν_3 frequencies of the crystalline samples, we believe that the missing signal of $tRNA_1^{Val}$ also must be in the 16–17-GHz range.

Excitation of $tRNA_1^{Val}$ at 335 nm is expected to generate the s^4U triplet state exclusively, and, indeed, transitions are seen that can easily be assigned as the ν_1 and ν_3 signals of s^4U.

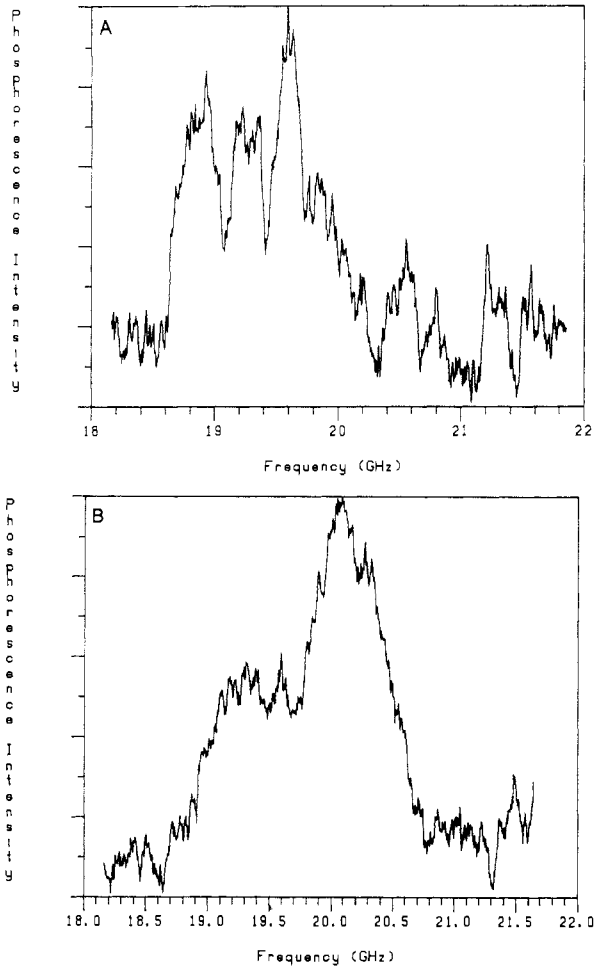

FIGURE 5: High-frequency ODMR transition of $tRNA_1^{Val}$ in EGW (50% v/v). Excitation wavelength is 335 nm, with emission monochromator set at 465 nm and a bandwidth of 3.2 nm. $T = 1.1$ K. Microwaves are swept from high to low frequencies at a rate of 39 MHz/ms. (A) Sample is dissolved in a Mg^{2+}-containing cacodylate buffer solution (pH 6.8). The signal results from signal averaging for 117 000 scans. (B) Sample is dissolved in a Mg^{2+}-free cacodylate buffer solution (pH 6.8), and signal results from signal averaging for 54 000 scans.

The low-frequency signal is structureless, while the ν_3 signal regions, presented in Figure 5, show resolved structure. The ν_3 region of the Mg^{2+}-containing sample, Figure 5A, shows a broad signal, which appears to be a composite of perhaps three partially resolved bands centered near 19.3 GHz. The Mg^{2+}-free sample, however, shows two sets of broad signals, Figure 5B, which are each unresolved envelopes of several different transitions, judging from their widths. The broad bands are centered at 19.2 and 20.0 GHz.

Other bases of tRNA contribute to the emission when 300-nm wavelength is used for excitation. Mg^{2+}-free and Mg^{2+}-containing samples both show similar ODMR transitions in the 0.7-GHz region. The low-frequency signal from the Mg^{2+}-free sample is shown in Figure 6. These samples also show ODMR transitions in the 5–6-GHz region. The signals in the 5–6-GHz region are shown in Figure 7. The ODMR response is a decrease in phosphorescence intensity for the Mg^{2+}-containing sample, whereas this response is an increase in intensity for the Mg^{2+}-free sample. The polarity of these signals was observed to be independent of observing wavelength, and the change in polarity appears to be associated with the presence or absence of Mg^{2+}. The low-frequency signal is very close to the ν_1 transition of thymine (Dinse & Maki, 1976), but the two high-frequency ODMR signals of thymine

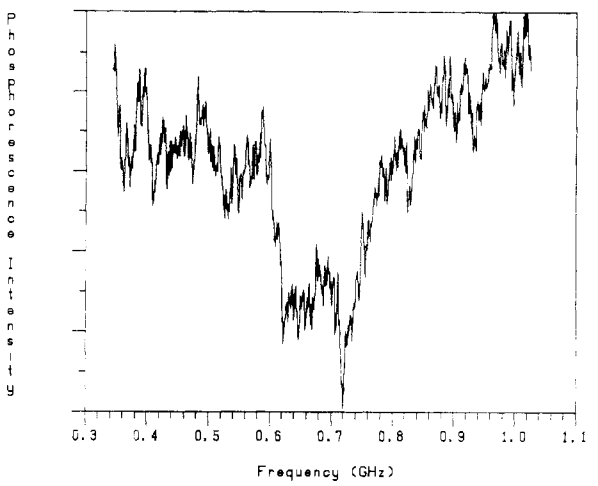

FIGURE 6: Low-frequency (ν_1) slow-passage ODMR transition of a long-lived triplet state in $tRNA_1^{Val}$ at 1.1 K in EGW (50% v/v). The solution is Mg^{2+}-free cacodylate buffer (pH 6.8). The sample is excited at 300 nm, with the emission monochromator set at 440 nm and a slit width of 1.6 nm. Microwaves are swept from low to high frequencies at a rate of 0.65 MHz/ms, and the signal is averaged over 23 000 scans.

have always been observed with comparable intensities. This is not the case for $tRNA_1^{Val}$ in which only one transition in the 5–6-GHz range is observed. The line width is too narrow to contain both the ν_2 and ν_3 signals which should be split by ca. 0.7 GHz.

(*C*) *Kinetics of the Triplet State.* The fast-passage transient method (Winscom & Maki, 1971) and the transient recovery method (Shain & Sharnoff, 1973) were used to study the kinetic parameters of the crystalline s^4U in U sample. Each of the two methods gives a single exponential decay curve with a decay lifetime of 13 ms upon exciting the ν_1 transition. The second method used on the ν_3 transition leads to a phosphorescence transient that can be deconvoluted into two exponential components with decay lifetimes of 1.4 and 23.9 ms. These values are very close to the individual sublevel lifetimes obtained (Taherian & Maki, 1981) for m^1s^4U, within experimental uncertainties. These values contain contributions from radiative and nonradiative processes. The radiative rates prove to be different in the two systems. From the ratio of the preexponential factors that give the relative radiative rate constants of the highest and lowest energy sublevels, we obtain 1:0.036 in s^4U and 1:0.086 in m^1s^4U for the relative radiative rate constants. These values clearly show a change in the radiative activity of the triplet sublevels of s^4U relative to m^1s^4U, although the total decay constants are approximately the same.

Discussion

(*A*) *Phosphorescence Spectra.* The phosphorescence spectra of $tRNA_1^{Val}$ at 1.1 K show more resolution when compared with the results reported at 77 K (Hélène et al., 1968; Hélène & Yaniv, 1970). This enables us to get more structural information from the spectra. In particular, the effect of Mg^{2+} ion on the phosphorescence spectrum is very easily seen from Figure 4. The presence of this ion has been shown to be required for biological activity and for stability of the native three-dimensional structure of tRNA (Beardsley & Cantor, 1970; Beardsley et al., 1970; Eisinger et al., 1970; Robinson & Zimmerman, 1971). The lack of Mg^{2+} ion, however, is not sufficient to cause complete disruption of tertiary base pairing of tRNA (Reid & Robillard, 1975). The reduced resolution of the s^4U phosphorescence in the Mg^{2+}-free sample can be

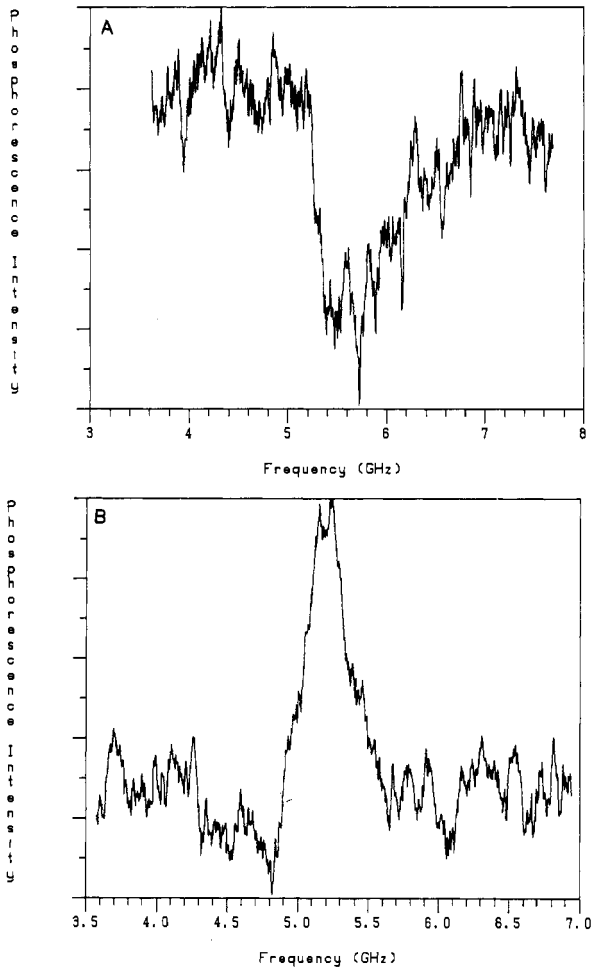

FIGURE 7: High-frequency slow-passage ODMR transition of a long-lived triplet state of $tRNA_1^{Val}$ at 1.1 K. The tRNA is dissolved in EGW (50% v/v) containing pH 6.8 cacodylate buffer. (A) Mg^{2+}-containing sample is excited at 300 nm and monitored at 465 nm with a monochromator slit width of 1.6 nm. The microwaves are swept from low to high frequencies at a rate of 4.7 MHz/ms. The signal is averaged over 27 000 scans. (B) Mg^{2+}-free sample is excited at 300 nm and monitored at 440 nm with a monochromator slit width of 1.6 nm. Microwaves are swept from low to high frequencies at a rate of 8.4 MHz/ms. The signal is averaged over 7200 scans.

attributed to the role of Mg^{2+} ion in stabilizing the structure of tRNA. In the absence of this ion, there might be a relatively continuous distribution of three-dimensional structures that differ from one another in subtle ways such as the relative orientation of some of the bases. This may be enough to cause small differences in the microenvironment of s^4U in different tRNA molecules, which in turn leads to broadening of the phosphorescence emission in the Mg^{2+}-free sample.

The long-lifetime, shorter wavelength emission, on the other hand, shows more resolved structure. Here again, reduced resolution in the Mg^{2+}-free sample can be attributed to the structural role of Mg^{2+} ion. The increase in relative intensity of long- to short-lived emissions, which results from the removal of Mg^{2+} ion, may be the result of a decrease in the efficiency of energy transfer to s^4U. Energy transfer efficiency varies with relative orientation of the chromophores (Siegel & Goldstein, 1965), as well as strongly with their separation. It is perhaps more reasonable to assume that orientational changes are responsible for this effect, because the presence of tertiary structures is a good indication that distance changes should not be too large. It should also be noted that solvent quenching can play an important role here, because in Mg^{2+}-free solution, s^4U is more accessible to small molecules such as methylmercury hydroxide (Maguire, 1976). This indicates that in the Mg^{2+}-free conformation the s^4U is more readily susceptible to solvent-quenching effects.

(B) ODMR. A comparison of the ν_3 signals of $tRNA_1^{Val}$ in the presence and absence of Mg^{2+} ion again shows the effect of this ion on the structure of tRNA. The Mg^{2+}-containing sample has a ν_3 ODMR spectrum that contains a group of partially resolved bands centered at 19.3 GHz. This heterogeneous appearance is due to a variation in $|D|$, since the $2|E|$ transition is relatively narrow and unstructured. It may be associated with structural flexibility, which is a characteristic feature of tRNA molecules (Schimmel & Redfield, 1980). The Mg^{2+}-free sample, on the other hand, shows two sets of signals that are unresolved and centered at 19.2 and 20.0 GHz. The 19.2-GHz peak is in the same general region as the ν_3 signal of the Mg^{2+}-containing sample. The presence of the second broad signal in Mg^{2+}-free tRNA at 20.0 GHz can be associated with a rather different s^4U environment in the sample. Possibly the signal centered at 19.2 GHz can be associated with a conformation similar to that of the Mg^{2+}-containing sample, while the band at 20.0 GHz may be cautiously assigned to a conformation with distinct structural differences. Evidence in favor of such possibility is the phosphorescence spectra of the two samples. A close comparison of the phosphorescence spectra in Figure 4 suggests that the Mg^{2+}-free spectrum may be a superposition of normal emission, having the same origin as that of the Mg^{2+}-containing sample, and a second emission which is red shifted by about 10 nm. At high temperatures in solution, the tRNA molecule probably undergoes dynamic structural fluctuations, and it is only in the process of freezing the solution that the more stable structures are immobilized and give rise to the observed heterogeneity of the ν_3 signals. Reduced biological activity of tRNA in the absence of Mg^{2+} indicates that conformational differences exist at room temperature.

As mentioned earlier, the complex structure of the ν_3 signal, compared with the ν_1 transition, reveals a greater sensitivity of the ZFS D parameter to environmental changes than of E. This means that the perturbations of the electronic wave functions are primarily affecting the properties of the triplet state along one of the principal magnetic axes. This same high sensitivity of the D parameter to the environment is largely responsible for the width of the ν_2 and ν_3 transitions of s^4U in the U host crystal. While the ν_1 transition is only 30 MHz wide, the ν_3 signal is as broad as 500 MHz, which is unusually large for crystalline samples. Crystalline hosts usually give rise to much narrower signals (Zuclich et al., 1974), and if the substitution in the unit cell is not unique, one might expect more than one narrow transition with frequency differences that are related to the extent of environmental effects.

The ODMR transitions originating from the long-lived emission occur at frequencies that are characteristic of pyrimidine bases (Maki, 1981). Thymine at position 54 is not likely to be the source of these ODMR signals, based on the occurrence of only one of the high-frequency signals. Uridine ODMR signals are not observed in polynucleotides due to a low intersystem crossing yield and high triplet energy leading to quenching of the triplet state. The ZFS is known to be very similar to that of thymine, however (Maki, 1981). Cytosine also has a high triplet energy, and triplet quenching by other bases is efficient (Eisinger & Lamola, 1971). The most probable candidate for the ODMR signals is cmo^5U which is located in the first position of the anticodon (Figure 1) (Sprinzl et al., 1978). The three-dimensional structure of tRNA is such that this part of the molecule protrudes from the more crowded

region containing the s^4U. On the basis of separation, cmo^5U has less probability of energy transfer to s^4U. On the other hand, except for the small difference in substitution at the 5 position, this base is identical with thymine, and the similar ODMR frequencies (Dinse & Maki, 1976) suggest this assignment.

(*C*) *Triplet Kinetics.* The difference in relative radiative rate constants of the sublevels involved in the ν_3 ODMR transition of s^4U in U compared with m^1s^4U in m^1U is larger than can be attributed to experimental uncertainties. This difference is also reflected in the average phosphorescence quantum yield ($\bar{Q}_p$) of these compounds. For m^1s^4U in m^1U, the maximum possible value of $\bar{Q}_p$ was estimated (Taherian & Maki, 1981) to be 0.24, while the 77 K measured values of s^4U and $m^1m^3s^4U$ are 0.16 (Shalitin & Feitelson, 1976b) and 0.30 (Lancelot, 1976), respectively. Since the total decay lifetimes remain nearly constant, these differences are directly related to phosphorescence quantum yields of individual sublevels (Taherian & Maki, 1981), if the reasonable assumption of equal triplet yields is made. Without a knowledge of the radiative properties of the intermediate sublevel that is involved in the ν_2 transition, a quantitative comparison is not possible, but there is enough evidence pointing to lower radiative and higher nonradiative activity of s^4U relative to m^1s^4U. Rearrangement of the radiative properties of s^4U is also manifested in the sign reversal of the ν_2 transition, which appears as a decrease in light intensity in this molecule.

There are two major differences between m^1s^4U and s^4U that may be responsible for their different radiative behavior. These are (a) the presence or absence of a bulky sugar group and (b) greater deviation from planarity in s^4U (Hawkinson, 1975). Ribose contains polar groups which can come very close to the chromophore in the three-dimensional structure. The interactions between the polar groups on the sugar and the π system of s^4U can affect the radiative properties of s^4U. Alternatively, when s^4U is part of a biopolymer, the sugar moiety can change the stacking interactions between neighboring molecules, which can account for a change in nonradiative rates.

Deviations from planarity are expected to have even larger influence on the properties of the triplet state. The sulfur atom deviations from the ring plane in neat crystals of s^4U and m^1s^4U are 0.18 (Saenger & Scheit, 1970) and 0.091 Å (Hawkinson, 1975), respectively. Although these distortions may be partly due to crystal packing (Hawkinson, 1975), differences in the sulfur coordinates in the crystals could reflect a different degree of nonplanarity in these two molecules. In recent work (M.-R. Taherian, W. H. Fink, and A. H. Maki, unpublished results) we have shown that deviations from planarity have an important influence on the mechanism of m^1s^4U emission. In nonplanar molecules there is no rigorous distinction between σ and π molecular orbitals, and the states become altered to have mixed characters. Since the radiative activity of triplet sublevels is determined by the oscillator strength of the singlet states which are mixed through spin–orbit coupling, nonplanarity is expected to influence the triplet sublevel decay rates.

Acknowledgments

We thank Professor P. R. Schimmel for communicating his results on the sequence of *E. coli* MRE 600 $tRNA_1^{Val}$.

References

Ballini, J.-P., Vigny, P., Thomas, G., & Favre, A. (1976) *Photochem. Photobiol. 24*, 321–329.

Beardsley, K., & Cantor, C. R. (1970) *Proc. Natl. Acad. Sci. U.S.A. 65*, 39–46.

Beardsley, K., Tao, T., & Cantor, C. R. (1970) *Biochemistry 9*, 3524–3532.

Crothers, D. M., Cole, P. E., Hilbers, C. W., & Shulman, R. G. (1974) *J. Mol. Biol. 87*, 63–88.

Dinse, K. P., & Maki, A. H. (1976) *Chem. Phys. Lett. 38*, 125–129.

Doctor, B. P., Loebel, J. E., Sodd, M. A., & Winter, D. B. (1969) *Science (Washington, D.C.) 163*, 693–695.

Eisinger, J. (1971) *Biochem. Biophys. Res. Commun. 43*, 854–861.

Eisinger, J., & Lamola, A. A. (1971) in *Excited States of Proteins and Nucleic Acids* (Steiner, R. F., & Weinryb, I., Eds.) pp 107–198, Plenum Press, New York.

Eisinger J., Feuer, B., & Yamane, T. (1970) *Proc. Natl. Acad. Sci. U.S.A. 65*, 638–644.

Elion, G. B., Ide, W. S., & Hitchings, G. H. (1946) *J. Am. Chem. Soc. 68*, 2137–2140.

Favre, A., Yaniv, M., & Michelson, A. M. (1969) *Biochem. Biophys. Res. Commun. 37*, 266–271.

Gauss, D. H., Grüler, F., & Sprinzl, M. (1979) *Nucleic Acids Res. 6*, r1–r19.

Hawkinson, S. W. (1975) *Acta Crystallogr., Sect. B B31*, 2153–2156.

Hélène, C., & Yaniv, M. (1970) *Eur. J. Biochem. 15*, 500–504.

Hélène, C., Yaniv, M., & Elder, J. W. (1968) *Biochem. Biophys. Res. Commun. 31*, 660–664.

Kim, S. H., Suddath, F. L., Quigley, G. J., McPherson, A., Sussman, J. L., Wang, A. H. J., Seeman, N. C., & Rich, A. (1974) *Science (Washington, D.C.) 185*, 435–440.

Lancelot, G. (1976) *Mol. Phys. 31*, 241–254.

Maguire, R. J. (1976) *Can. J. Biochem. 54*, 583–587.

Maki, A. H. (1981) in *Triplet State ODMR Spectroscopy: Techniques and Applications to Biophysical Systems* (Clarke, R. H., Ed.) Wiley, New York (in press).

Maki, A. H., & Co, T. (1976) *Biochemistry 15*, 1229–1235.

Maki, A. H., Svejda, P., & Huber, J. R. (1978) *Chem. Phys. 32*, 369–380.

McCloskey, J. A., & Nishimura, S. (1977) *Acc. Chem. Res. 10*, 403–410.

Pochon, F., Balny, C., Schert, K. H., & Michelson, A. M. (1971) *Biochim. Biophys. Acta 228*, 49–56.

Reid, B. R., & Robillard, G. T. (1975) *Nature (London) 257*, 287–291.

Robertus, J. D., Ladner, J. E., Finch, J. T., Rhodes, D., Brown, R. S., Clark, B. F. C., & Klug, A. (1974) *Nature (London) 250*, 546–551.

Robinson, B., & Zimmerman, T. P. (1971) *J. Biol. Chem. 246*, 110–117.

Saenger, W., & Scheit, K. H. (1970) *J. Mol. Biol. 50*, 153–169.

Schimmel, P. R., & Redfield, A. G. (1980) *Annu. Rev. Biophys. Bioeng. 9*, 181–221.

Shain, A. L., & Sharnoff, M. (1973) *J. Chem. Phys. 59*, 2335–2343.

Shalitin, N., & Feitelson, J. (1973) *J. Chem. Phys. 59*, 1045–1051.

Shalitin, N., & Feitelson, J. (1976a) *Biochemistry 15*, 2092–2097.

Shalitin, N., & Feitelson, J. (1976b) in *Excited States of Biological Molecules* (Birks, J. B., Ed.) pp 190–198, Wiley-Interscience, New York.
Siegel, S., & Goldstein, L. (1965) *J. Chem. Phys. 43*, 4185–4187.
Singhal, R. P., & Fallis, P. A. M. (1979) *Progr. Nucleic Acid Res. Mol. Biol. 23*, 227–290.
Sprinzl, M., Grüter, F., & Gauss, D. H. (1978) *Nucleic Acids Res. 5*, r15–r27.
Steiner, R. F., Miller, D. B., & Heerman, K. C. (1967) *Arch. Biochem. Biophys. 120*, 464–467.
Taherian, M.-R., & Maki, A. H. (1981) *Chem. Phys. 55*, 85–96.
Teeter, M. M., Quigley, G. J., & Rich, A. (1980) in *Nucleic Acid-Metal Ion Interactions* (Spiro, T. G., Ed.) pp 145–177, Wiley-Interscience, New York.
Walker, R. T., & RajBhandary, U. L. (1970) *Biochem. Biophys. Res Commun. 38*, 907–914.
Winscom, C. J., & Maki, A. H. (1971) *Chem. Phys. Lett. 12*, 264–268.
Wong, K. L., & Kearns, D. R. (1974) *Nature (London) 252*, 738–739.
Wong, K. L., Bolton, P. H., & Kearns, D. R. (1975) *Biochim. Biophys. Acta 383*, 446–451.
Yaniv, M., & Barrell, B. G. (1969) *Nature (London) 222*, 278–279.
Zuclich, J., von Schütz, J. U., & Maki, A. H. (1974) *J. Am. Chem. Soc. 96*, 710–714.

Secondary Structure of Prokaryotic 5S Ribosomal Ribonucleic Acids: A Study with Ribonucleases†

Steve Douthwaite and Roger A. Garrett*

ABSTRACT: The structures of 5S ribosomal RNAs from *Escherichia coli* and *Bacillus stearothermophilus* were examined by using ribonucleases A, T_1, and T_2 and a double helix specific cobra venom ribonuclease. By using both 5′- and 3′-^{32}P-end labeling methods and selecting for digested but intact 5S RNA molecules, we were able to distinguish between primary and secondary cutting positions and also to establish the relative degree of cutting. The data reveal the predicted similarities of the higher order structure in the two RNAs but also demonstrate a few significant differences. The data also provide direct evidence for three of the helical regions of the Fox and Woese model of 5S RNA [Fox, G. E., & Woese, C. (1975) *Nature (London) 256*, 505] and support other important structural features which include a nucleotide looped out from a helical region which has been proposed as a recognition site for protein L18.

5S RNA is the smallest ribosomal RNA and is an integral part of the large ribosomal subunit. Although its function in protein biosynthesis remains unknown, it has been located by immunoelectron microscopy and reconstitution experiments in a region of the 50S subunit interface known to be associated with peptidyltransferase activity (Stöffler et al., 1980; Dohme & Nierhaus, 1976). The relative structural simplicity of 5S RNA has rendered it an obvious choice for studies on both ribosomal RNA secondary structure and the chemistry and specificity of protein–RNA interactions. A base-pairing scheme common to all prokaryotic 5S RNAs, consisting of four double-helical regions, was first proposed by Fox & Woese (1975) on the basis of comparative sequence studies. This almost certainly constitutes the minimum amount of base pairing in the 5S RNA since several lines of evidence indicate that the remainder of the RNA is also highly structured. For example, only 4 out of the remaining 21 "unpaired" guanines in the *Escherichia coli* RNA structure are strongly modified by kethoxal (Noller & Garrett, 1979) and a large region (nucleotides 69–87 and 89–110) is highly resistant to ribonuclease A (Douthwaite et al., 1979).

The object of the present study was to exploit the new rapid RNA gel sequencing technology to investigate the topography of the A form of 5S RNA by using ribonucleases of different specificities. Ribonucleases A, T_1, and T_2 have a strong preference for single-stranded regions, and the *Naja naja oxiana* cobra venom ribonuclease is specific for double-helical structures (Vassilenko & Babkina, 1965).

In earlier studies with ribonucleases A, T_1, and T_2, cutting positions have generally been assumed to occur in accessible, non-base-paired regions (Monier, 1974). However, this interpretation is subject to the criticism that a primary cut may produce a structural rearrangement which results in a secondary cut occurring at a position which is not accessible in the native structure. In the present study, we have tried to overcome this problem first by performing very mild digests and then selecting, electrophoretically, for intact 5S RNA molecules with a few nicks. Second, we have employed both 3′- and 5′-end-labeled RNA which generally enables us to distinguish between primary and secondary cuts. We have then analyzed the positions and intensities of the cuts over a range of enzyme conditions, on rapid sequencing gels. The structures of two ribosomal 5S RNAs, from *E. coli* and *Bacillus stearothermophilus*, were examined and special attention was given to common features. A fairly detailed picture emerges of the RNA structure; the data provide experimental support for the base-pairing scheme of Fox & Woese (1975) and yield further insight into the structure of the other RNA regions.

Materials and Methods

5S RNA was isolated from *E. coli* strain MRE 600 and *B. stearothermophilus* strain NCA 1503, following the general

† From the Division of Biostructural Chemistry, Kemisk Institut, Aarhus Universitet, DK-8000 Aarhus C, Denmark. *Received June 4, 1981*. This work was supported by a temporary research grant from the Danish Research Council. S.D. gratefully received support from Aarhus University, the Deutsche Forschungsgemeinschaft, the Max-Planck-Institut für Molekulare Genetik in West Berlin, and EMBO.

0006-2960/81/0420-7301$01.25/0